Chapter 3

Isolation and screening of *Diplosphaera mucosa VSPA* for bioremediation of textile and carpet effluent

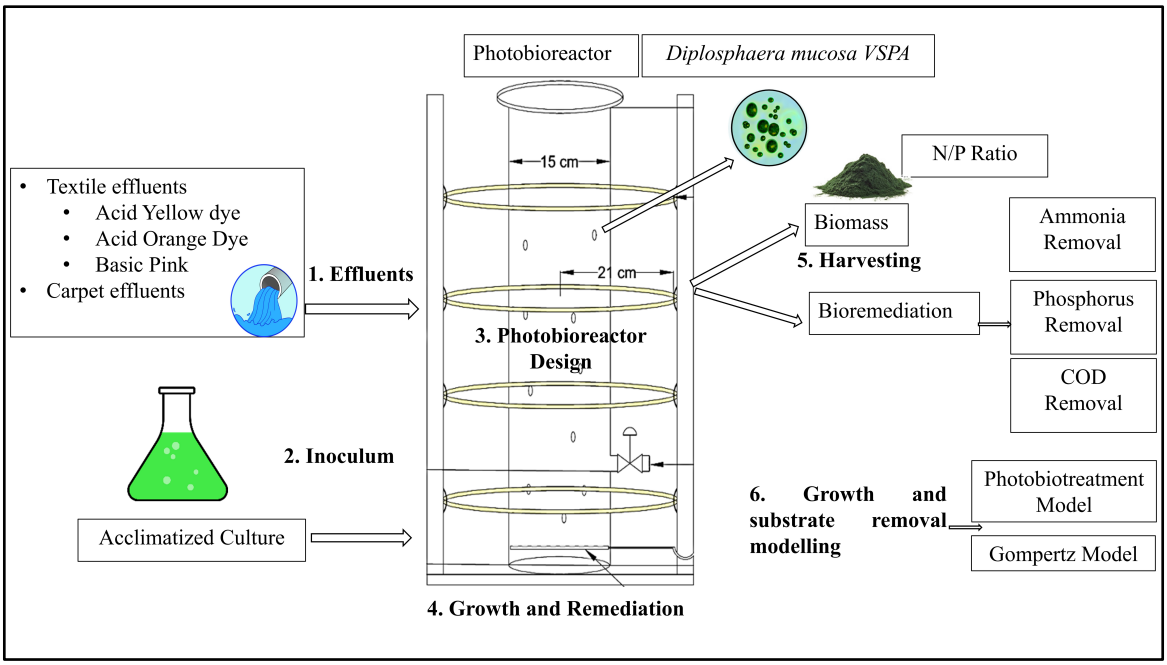

Isolation and preliminary screening of *Diplosphaera mucosa VSPA* for bioremediation of textile and carpet effluent

3.1. Introduction

The current study assessed the potential of one of these understudied species, considering the points mentioned, Diplosphaera mucosa, belonging to the class Trebiouxyphyceae, for treating carpet and textile effluent. A web of knowledge database search reported no publication related to the carpet and textile effluent treatment by Diplosphaera mucosa. The treatment process was carried out in a 10-liter bubble column photobioreactor with a discussion of its design parameters. The design parameters discussed in the present study were the volumetric mass transfer coefficient, hydrodynamic properties, and light uptake rate. Biomass production and treatment efficiency of the Diplosphaera mucosa were compared with those of a well-known strain of the same class, Chlorella pyrenoidosa. The comparison will indicate whether the application of Diplosphaera mucosa for wastewater treatment will be feasible or not. The pattern of growth and substrate removal in the photobioreactor was described using the Photobiotreatment Model (PhBT) and Gompertz Model (GP). The impact of wastewater's N/P ratio on biomass generation has also been explored and can be used as a critical design factor for reactor operation.

3.2. Methodology

3.2.1. Isolation and characterisation of strains

Diplosphaera mucosa strain was isolated from the inlet Sewage Treatment Plant (STP) in Bhagwanpur, Varanasi, India (25° 16' 21" N, 83° 0' 16.92" E). The sample was serially diluted and spread on agar plates containing Bold Basal Media (BBM) (Bischoff 1963). Plates were kept in an incubator at 25 °C and illuminated at 2500 lux intensity using LED tubes. Single colonies were picked up by examination under the microscope and streaked on fresh plates. The streaking process continued until a pure culture (free from

contamination, confirmed under the microscope) was obtained. The sequence of the isolated culture was identified by 18s rRNA sequencing and analysed by the BLAST program. Analysis revealed that the strain showed close similarity with *Diplosphaera mucosa* (89.60%) and was therefore named *Diplosphaera mucosa VSPA*. The sequencing process was assisted by the National Collection of Industrial Microorganisms (NCIM), National Chemical Laboratory (NCL), Pune, India. A *Chlorella pyrenoidosa* strain was also procured from the NCIM. Its revival and cultivation steps have been explained in the supplementary section (S2.1)[268].

3.2.2. Collection and characterisation of industrial effluents

Textile wastewater was collected from local textile industries in Varanasi, India (25° 18' 0" N, 82° 55' 48" E). Three variants of textile wastewater were collected: (a) Textile effluent containing acid yellow dye (TE1); (b) Textile effluent containing acid orange dye (TE2); (c) Textile effluent containing basic pink dye (TE3). Carpet industry effluent was collected from the Carpet Industry in Bhadohi, India (25° 22' 48" N, 82° 35' 24" E). The temperature of the wastewater samples was measured at the site of collection. The wastewater samples were filtered and put into storage for further use at 4 °C. Utilising standardised and globally accepted techniques, various wastewater sample parameters, including nitrogen, phosphorus, COD, and BOD, were determined [269]. Important sample parameters involved in the study are presented in **Table 3.1**.

Table 3.1. Characterisation of different effluents through standard procedures[268].

S.No.	Parameter	Textile industry effluents			Carpet industry effluents	Legally admissible limit (Organization 2022)
		TE1	**TE2**	**TE3**		
1.	Colour (Visual)	Yellow	Orange	Dark Pink	Reddish brown	Colourless
2.	pH	8.1±0.16	8.2±0.16	8.2±0.24	8.1±0.08	6.5-8.5
3.	Temperature (^{0}C)	35±1.63	35±0.81	38±0.81	35±1.24	NA
4.	Turbidity (NTU)	13.2±0.16	14.3±0.24	15.6±0.32	210±7.34	<1
5.	Nitrogen (ammonia)(mg/L)	45.2±2.44	54.6±3.26	46.2± 3.26	82.8 ±1.63	0.2
6.	Nitrogen (Nitrate)(mg/L)	2.8±0.16	2.12±0.03	2.5±0.24	3.5 ±0.24	50
7.	Phosphate (mg/L)	5.4±0.32	6.3±0.16	7.8±0.73	9.3±2.44	0.1
8.	N/P ratio	8.3±0.24	8.6±0.32	5.92±0.57	9.0±0.32	NA
9.	Dissolved oxygen(mg/L)	3.8±0.32	1.6±0.24	2.8±0.32	1.6±0.16	6.5-8
10.	BOD_5 (mg/L)	78.8±4.89	87.2±3.26	83.6±3.75	104±6.53	1-2
11.	COD (mg/L)	396±16.32	372±16.32	438±14.69	1570±16.32	10
12.	Color (Hazen)	142±3.26	180±9.79	202±9.79	96±4.08	NA

3.2.3. Photobioreactor construction

A cylindrical bubble column PBR was constructed using an acrylic tube purchased from a local hardware shop (**Figure 3.1**). The total height of the reactor was 60 cm, with outer and inner diameters of 16 cm and 15 cm, respectively. The total volume of PBR was 10.6 L, with a working volume of 9 L. PBR was illuminated by four 30 W circular LED tube lights having a radius of 21 cm and providing 5000 lux intensity. The use of circular LED lights provides uniform light intensity around the reactor. A sampling port was provided at a height of 12 cm from the bottom. Aeration was done by an air compressor, and the sparger was placed at the bottom of the PBR. The bubble column PBR design parameters have been represented in **Table 3.2**.

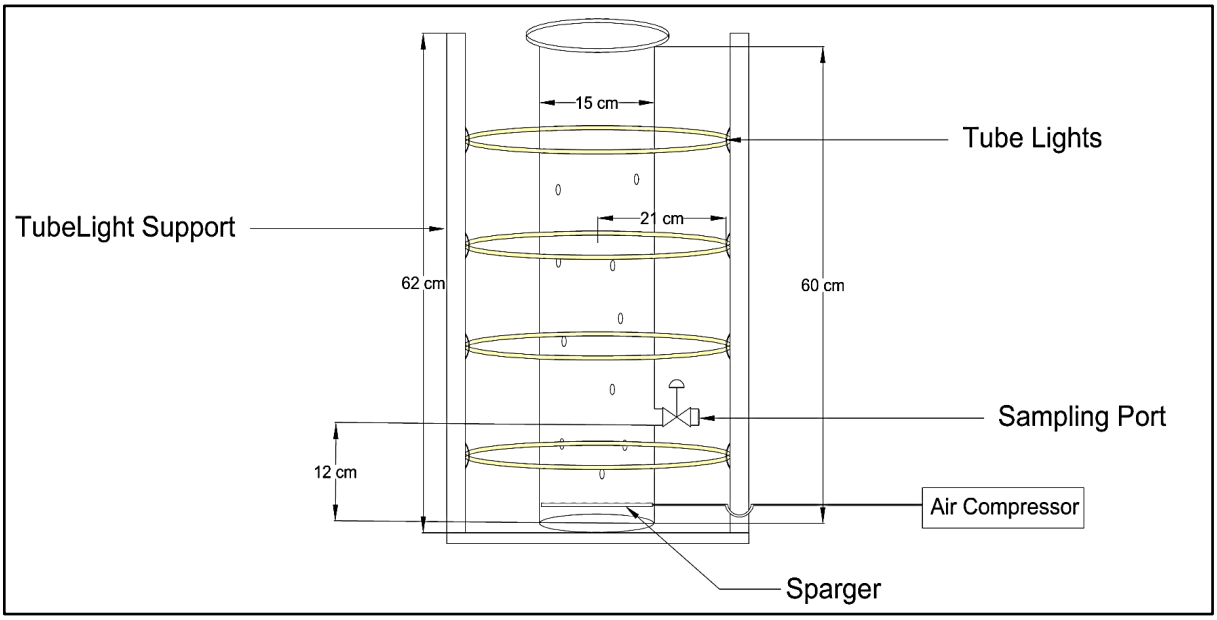

Figure 3.1. Simplified diagram of the conventionally designed bubble column photobioreactor used in the present study (Total height: 60 cm; Inner diameter: 16 cm; Outer diameter: 15cm). Circular tube lights (30 W each) were used for illumination, and aeration was done using an air compressor through a sparger. Sampling port was used for daily sample analysis. (Designed in AUTOCAD 2023 Student Version).

3.2.3.1. Light Intensity and Penetration Loss

The total luminous flux (φ_v) passing through the reactor was calculated using Eq. (3.1):

$$\varphi_v = P \times \eta \tag{3.1}$$

where, P stands for power in watts (W), and η indicates lumens per watt (lm/W).

3.2.3.2. Light uptake rate

The light uptake rate (q) was calculated using Eq. (3.2):

$$q = \frac{\varphi . I_o . A_o}{X} \tag{3.2}$$

where, I_o is the total incident irradiance μE/m^2-s, φ is the proportion of photosynthetically available light (%), X is the biomass concentration (g/L), and A_o is the total area of irradiance (m^2).

3.2.3.3. Volumetric mass transfer coefficient (K_La)

K_La is one of the most critical parameters for designing a photobioreactor. Under the same hydrodynamic conditions, the mass transfer coefficient (K_L) and the square root of the diffusivity (D) follow the penetration theory [270]. Microalgal density mainly depends on the mass transfer rate of O_2 and CO_2 across the gas-liquid interface. K_La (CO_2) is calculated using Eq. (3.3) [271]:

$$K_L a(CO_2) = \sqrt{\frac{D_{O_2}}{D_{CO_2}}} \times K_L a(O_2) \tag{3.3}$$

where, D_{O_2} and D_{CO_2} are 2 x 10^{-9} m^2/s and 2.41 x 10^{-9} m^2/s, respectively, at 298.15 K. K_La (O_2) can be calculated with the help of the dynamic gassing out technique method as shown by Eq. (3.4) [272]:

$$K_L a(O_2).(t - t_o) = \ln \frac{(C^* - C_o)}{(C^* - C)} \tag{3.4}$$

where, t and t_o are given and initial times, respectively, C_o indicates the initial dissolved concentration of O_2, C* indicates the saturated dissolved concentration of O_2, and C indicates the dissolved concentration of O_2 at the given time t.

3.2.3.4. Hydrodynamic property

Various hydrodynamic properties such as interfacial area, gas hold-up, bubble rise velocity, and bubble diameter also hold importance during PBR design.

Table 3.2. Different design parameters were derived for the design of a conventional photobioreactor.

S. No.	Design Parameter	Design value
1.	Height/ Diameter	4.064
2.	Cross sectional area	0.017 m^2
3.	Volume of reactor	0.0108 m^3
4.	Light intensity	36.45 $\mu mol.m^{-2}\ s^{-1}$
5.	Light uptake	1.28 $\mu mol\ s^{-1}\ (g/L)^{-1}$
6.	Airflow rate	0.2 vvm
7.	Gas holds up (Ɛ)	Ɛ= 0.0115
8.	Bubble diameter	d_b= 0.0028 m
9.	Reynolds no. (Re)	933
10.	Superficial gas velocity	U_G= 0.078 m s^{-1}
11.	Bubble rise velocity	U_b=0.8 m s^{-1}
12.	Interfacial area (a)	a=29.9 m^2

3.2.4. Experimental Procedure

Batch experiments were performed in conventionally designed PBR to determine both strains' pollutant removal efficiency (ammonium nitrogen, phosphate phosphorus, COD, and colour) and biomass productivity. For inoculum preparation, strains were cultivated in 900 ml of BBM (10% of the reactor working volume) and monitored till the culture reached the mid-log phase by measuring optical density at 680 nm. After that, the growing strains were used for inoculating the reactor filled with effluent. pH was monitored daily by measuring the pH of the samples withdrawn from the reactor and maintained at 7 using 1N

HCl and 1N NaOH. Light intensity was maintained at 5000 lux intensity via an electric regulator, and the 12 h:12 h light/dark cycle was maintained manually. Light intensity was measured using a lux meter. The temperature of the chamber in which the reactor was kept was maintained at 25 ^{o}C by an air conditioner and measured by dipping a mercury thermometer in the reactor. Air in the reactor was sparged at 3 L/minute through an air compressor. The reactor operated until the stationary phase was achieved, which took around 10 days. The stationary phase was determined by measuring the optical density of the samples withdrawn daily from the reactor. Samples were randomly withdrawn from the reactor for microscopic analysis to determine the presence of contamination by other microbes. The reactor without inoculum was also operated for 10 days, which served as control. All experiments were performed in triplicate, and average values and standard deviations were used for further calculation.

3.2.5. Analytical Techniques

Every day, a predetermined volume of culture was taken out of the sample port to track the production of biomass and the elimination of nutrients. By measuring the sample's absorbance (Abs) at 680 nm, the biomass concentration (Conc.) was calculated, as per Eq. (3.5) for *D. mucosa VSPA* and Eq. (3.5) for *C. pyrenoidosa*, respectively:

$$Abs. = 0.1324 \times Conc. \tag{3.5}$$

$$Abs. = 0.1765 \times Conc. \tag{3.6}$$

These equations were derived experimentally by plotting a standard curve between absorption and the known concentration of biomass. Using the above biomass concentration value, biomass productivity and specific growth were calculated by Eq. (3.7) and (3.8), respectively [273]:

$$P = \frac{X_f - X_i}{t_f - t_o} \tag{3.7}$$

$$\mu = \frac{lnX_t - lnX_o}{t_{f-t_o}} \quad (3.8)$$

where X_t (g L^{-1}) represents the biomass concentration at time t (d), Xo (g L^{-1}) represents the initial biomass concentration, t_f and t_o represent the final and initial sampling times, respectively, and μ (d^{-1}) represents the specific growth rate. In the 6th equation, *P* represents productivity (g L^{-1} d^{-1}), and X_i and X_f are the initial and final conc. of biomass (g L^{-1}), respectively, at times t_i and t_f. In addition to biomass concentration, chlorophyll (Chl) content was also determined, as sometimes debris or solids present in the reactor may hinder in accurate biomass determination.

A technique described by Lichtenthaler & Buschmann was used to determine the amount of chlorophyll in the microalgae[274] The sample was briefly diluted in 95% ethanol (HiMedia, India), filtered twice through filtered membranes, and centrifuged at 2,500 rpm for ten minutes. After the supernatant and pellet were separated, supernatant's absorbance was noted between 400 and 700 nm (Schimadzu UV-1800). Chl a, Chl b, and total carotene ($C_{(x+C)}$) all exhibit maximum absorbance at wavelengths of 664 nm, 648 nm, and 470 nm, respectively, according to Lichtenthaler & Buschmann (2001). All these experimental setups were carried out in triplicates. The chlorophyll content was estimated by the following equations [275]

$$\text{Chl a } (\mu g/ml) = (13.36 \times OD_{664}) - (5.19 \times OD_{648}) \quad (3.9)$$

$$\text{Chl b } (\mu g/ml) = (27.43 \times OD_{648}) - (8.12 \times OD_{664}) \quad (3.10)$$

$$C_{(x+c)} = (1000 \times OD_{470} - 2.13 \times Chla - 97.64 \times \text{Chl b})/ 209 \quad (3.11)$$

$$\text{Total chlorophyll} = Chla + \text{Chl b} \quad (3.12)$$

Next, samples were centrifuged at 8,000 rpm for 10 minutes to determine the nutrient level. After that, the pellet was discarded, and measurements were done using the

supernatant. NH_4^+-N and PO_4^{3-}-P concentrations were measured by the standard spectrophotometric method described by phenate and vanadomolybdophosphoric acid, respectively [269]. COD was measured by the close reflux titrimetric method [269]. After determining the nutrient values, the removal efficiency (RE) of the nutrients was determined by Eq. (12), respectively:

$$RE = \frac{N_o - N_f}{N_o} \times 100 \quad (3.13)$$

where RE indicates the percent removal efficiency, and N_f and N_o indicate the final and initial nutrient concentrations (mg L^{-1}).

3.2.6. Mathematical modelling study

For determining the growth and substrate removal patterns from the reactor and validating the experimental results, kinetic modelling studies are necessary. In the present work, two non-linear mathematical models, the photobiotreatment model (PhBT) and the Gompertz model, were used for the kinetic study. Models also assist in the reactor design and scale of the process. The PhBT model is the modified Verhult logistic model that assumes nutrient removal by microalgae depends on the biomass productivity of microalgae. In contrast, the Gompertz model assumes that nutrient removal does not depend on biomass productivity. Biomass concentration and substrate removal determined by the PhBT model are expressed by Eq.(13.1) and Eq.(13.2):

$$X = \frac{X_O X_m e^{pt}}{X_m - X_o + X_o e^{pt}} \quad (3.14)$$

$$S = \frac{\left(\frac{X_o}{Y} + S_o\right)(S_o - S_{na}) - S_{na}\left(S_o - \left(\frac{X_o}{Y} + S_o\right)\right)e^{pt}}{(S_o - S_{na}) - \left(S_o - \left(\frac{X_o}{Y} + S_o\right)\right)e^{pt}} \quad (3.15)$$

where, X (g/L) indicates the biomass concentration at time t, (days), X_o indicates the initial biomass concentration (g/L), X_m indicates the maximum biomass concentration (g/L), S (mg/L) indicates the substrate concentration at time t, S_o indicates the initial substrate concentration (mg/L), S_{na} indicates the non-assimilable substrate concentration

(mg/L), Y indicates the biomass yield (g/mg), and p indicates the maximum specific growth rate (day^{-1}). The Gompertz model for biomass and substrate is expressed by Eq. (14.1) and (14.2), respectively:

$$X = A \times \exp\left[-exp\left\{\left(\frac{\mu_m \times \exp(1)}{A}\right) \times (\lambda - t) + 1\right\}\right] \quad (3.16)$$

$$S(t) = S_i + \left(S_f - S_o\right) \times \exp[-\exp\{k \times (\lambda - t) + 1\}] \quad (3.17)$$

where, μ_m denotes the maximum specific growth rate (d^{-1}), λ is the lag time (d), A is the maximum biomass concentration (g/L), S(t) is the substrate or nutrient concentration (mg/L) at time t (d), and k is the nutrient uptake rate or substrate utilisation rate (d^{-1}).

3.2.7. Statistical Analyses

Experimental findings and error bars were plotted using Origin Lab (version 2017). The significance of the differences between the examined cultures was assessed using the Student's paired t-test. T-test was carried out using Orgin Lab (Version 2017) at a significance level of 0.05. The models were solved using a non-linear regression method using the solver supplement of Microsoft Excel. Kinetic parameters were determined by minimising the sum of square errors. The coefficient of regression (R^2) is not enough to evaluate the fair comparison of the models, as the values of R^2 are nearly similar. Therefore, another criterion, the second-order Akaike information criterion (AICC) test, was used for model comparison as expressed by Eq.(15). The model with a lower AICC value is suggested to be a better one.

$$AICC = Nln\left(\frac{RSS}{N}\right) + 2K + \frac{2K(K+1)}{N-K-1} \quad (3.18)$$

The sample size is denoted by N, the residual sum of squares is denoted by RSS, and the number of estimated parameters in the model is denoted by K.

3.3. Result and Discussion

3.3.1. Biomass Production

Algal biomass is thought to be a potentially useful resource to produce biofuels. Identifying and improving factors that enhance the growth rate and higher lipid content makes microalgae an attractive tool for biofuel production. The nutrients in the wastewater are utilised by the microalgal species and assimilated for biomass production and product formation. **Table 3.3** represent a comparative evaluation of the biomass production for *D. mucosa* VSPA and *C. pyrenoidosa* in different wastewater effluents. In all cases, *D. mucosa VSPA* has higher biomass productivity (1.2-1.5 folds) than *C. pyrenoidosa* ($p < 0.05$). *Diplosphaera* species were first isolated by P.A. Broady from Antarctic terrestrial habitats in 1983 [276]. Therefore, due to the source of their isolation, *Diplosphaera* species may easily adapt to the unfavourable environment of wastewater, leading to high biomass productivity. As per **Figure 3.2**, nearly two days of lag phase were obtained in all effluents, possibly due to toxic elements in wastewater (mostly Azo dyes) [277]. Therefore, microalgal species need some time to acclimate themselves to wastewater environments. Microbes adapt to the unfavourable environment of wastewater during the lag phase through various physiochemical changes, such as the creation of enzymes needed to assimilate substrates present in the medium [236]. The stationary phase in all textile effluents for both species was obtained earlier than carpet effluent due to a lower nutrient concentration in textile effluents, around the 8^{th} day. In carpet effluent, the stationary phase was observed after the 9^{th} day.

Table 3.3. Biomass and chlorophyll concentrations obtained during the cultivation of *D. mucosa* VSPA and *C. pyrenoidosa* in different effluents.

Wastewater Source	N/P Ratio	*D. mucosa* VSPA			*C. pyrenoidosa*		
		Biomass concentration (g/L)	Chl a (µg/ml)	Chl b (µg/ml)	Biomass concentration (g/L)	Chl a (µg/ml)	Chl b (µg/ml)
TE1	8.37± 0.8	3.98± 0.2	2.98± 0.2	0.89± 0.1	3.31± 0.2	2.68± 0.2	1.08± 0.24
TE2	8.6± 0.6	3.85± 0.3	2.76± 0.15	1.06± 0.14	3.00± 0.6	2.86± 0.24	1.09± 0.34
TE3	5.92± 0.9	2.90± 0.32	2.82± 0.14	1.12± 0.24	2.28± 0.5	2.72± 0.21	1.08± 0.21
Carpet Effluents	9.01± 0.8	4.26± 0.24	3.72± 0.6	1.34± 0.26	4.02± 0.24	3.52± 0.3	1.24± 0.18

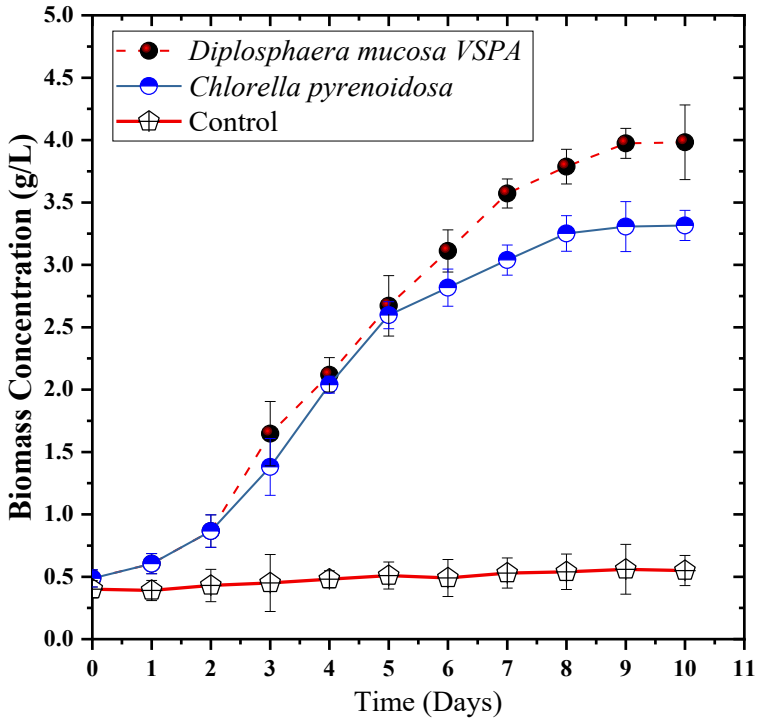

(A) Textile Effluents (TE1)

Figure 3.2. The pattern of biomass concentration obtained during the cultivation of *D. mucosa* VSPA (Red dashed line) and *C. pyrenoidosa* (Blue dashed line) in Textile Effluent 1; The red solid line represents the control. Approximately two days into the log phase, and the stationary phase was achieved after the 8th day.

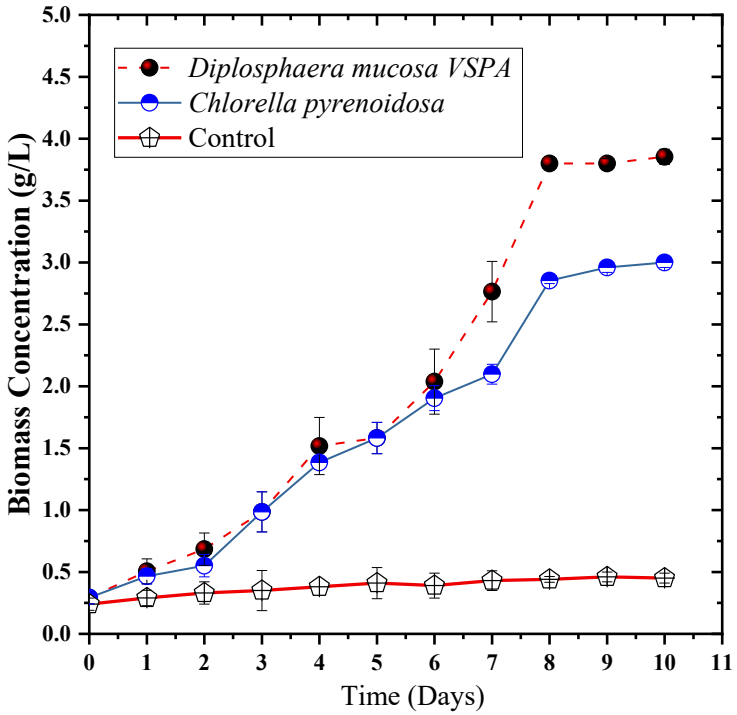

(B) Textile Effluents (TE2)

Figure 3.3. The pattern of biomass concentration obtained during the cultivation of *D. mucosa* VSPA (Red dashed line) and *C. pyrenoidosa* (Blue dashed line) in Textile Effluent 2; The red solid line represents the control. Approximately two days into the log phase, and the stationary phase was achieved after the 8th day.

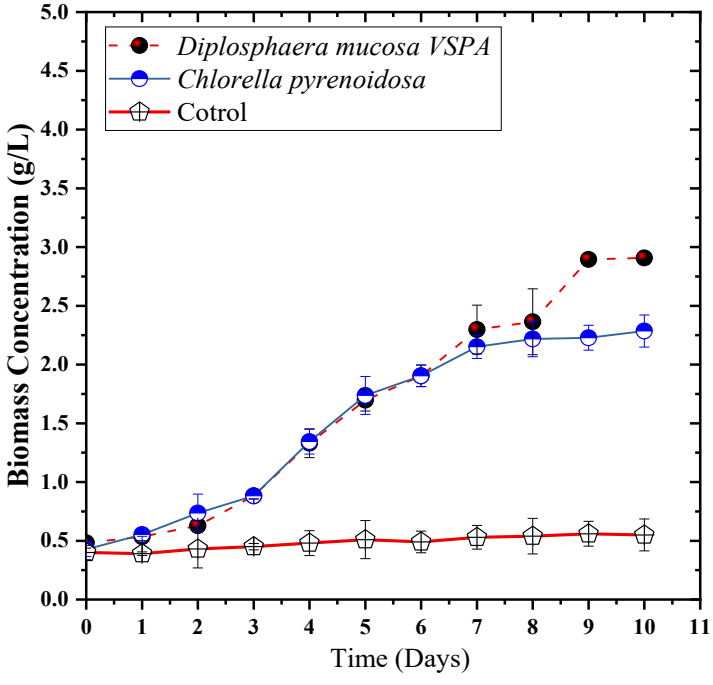

(C) Textile Effluents (TE3)

Figure 3.4. The pattern of biomass concentration obtained during the cultivation of *D. mucosa* VSPA (Red dashed line) and *C. pyrenoidosa* (Blue dashed line) in Textile Effluent 3; The red solid line represents the control. Approximately two days into the log phase, and the stationary phase was achieved after the 8th day.

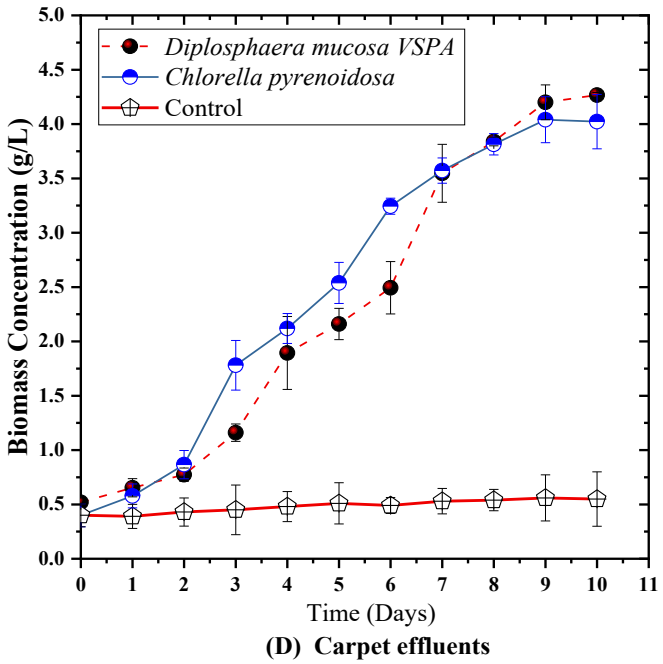

Figure 3.5. The pattern of biomass concentration obtained during the cultivation of *D. mucosa* VSPA (Red dashed line) and *C. pyrenoidosa* (Blue dashed line) in Carpet Effluent; The red solid line represents the control. Approximately two days into the log phase, and the stationary phase was achieved after the 8th day.

The highest biomass concentration was obtained in the case of carpet effluent, which was 4.26 g/L in *D. mucosa* VSPA culture and 4.02 g/L in *C. pyrenoidosa* culture. Among the three variants of textile wastewater, the highest biomass concentration of 3.98 g/L was obtained in TE1 by *D. mucosa* VSPA. In contrast, the lowest biomass concentration of 2.20 g/L was obtained in TE3 by *C. pyrenoidosa*. The reason for such a trend in biomass production is the high N/P ratio of carpet effluent. Based on Redfield's work, the typical stoichiometric formula of the microalgal biomass is $C_{106}H_{181}O_{45}N_{16}P$. As a result, the N/P ratio of the culture medium should be around 16:1 to obtain high biomass productivity

[235].The highest N/P ratio of 9.01:1 was detected in carpet effluent. Another reason can be the presence of azo dyes in textiles that inhibit microalgae growth. Among the three variants of textile effluent, the highest N/P ratio was detected in TE1, which was 8.37:1. The Same was reflected in the biomass production trend. Biomass productivity decreased or became nil when all effluents' N/P ratios reached below 5. In a 1.4 L laboratory-designed PBR, Wagner et al. (2021) evaluated the effects of various N/P ratios on the growth of *Chlorella sp.* during continuous cultivation. According to their findings, microalgae growth decreased when the N/P ratio was below 5.2:1 [234]. In another study, Mayers et al. (2014) cultivated *Nannochloropsis* sp. at various N/P ratios ranging from 16:1 to 80:1. 16:1 and 32:1 N/P ratios supported a high microalgae growth rate, but a decrease in growth rate was detected at 64:1 and 80:1 N/P ratios [233].

3.3.2. Pollutant Removal

Wastewater contains ample nutrients that support microalgae growth and metabolism[138]. A general diagram depicting the mechanism of nutrient removal by microalgae has been shown in **Figure 3.6.** Microalgal cells directly uptake ammonium nitrogen via the ammonium transporter. After that, glutamate and ATP facilitate the incorporation of NH_4^+-N into glutamine, which results in the formation of other amino acids and the generation of microalgae biomass[278]. Phosphorus is commonly present in wastewater as orthophosphate (PO_4^3-), which microalgae uptake via an active transport mechanism. This PO_4^3- gets incorporated into various organic compounds, such as ATP, through phosphorylation [279].

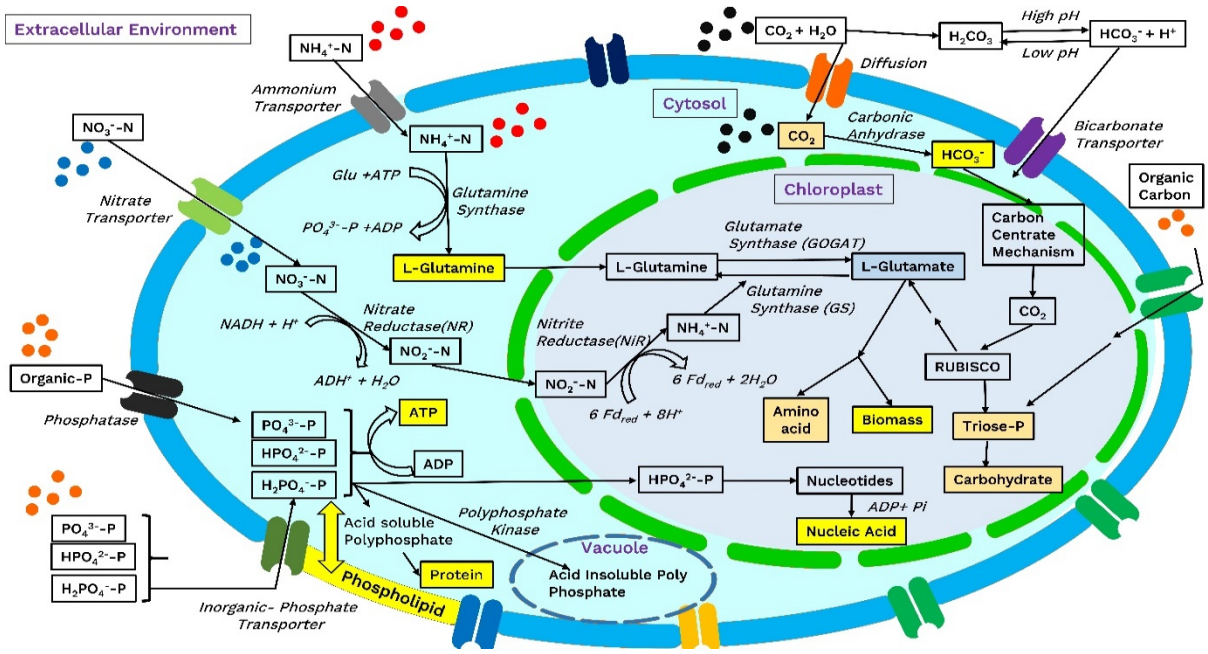

Figure 3.6. Schematic diagram representing the uptake of carbon, nitrogen and phosphorus by microalgal cells.

3.3.2.1. Ammonium nitrogen (NH_4^+-N) removal

Microalgal cells require less energy to uptake NH_4^+-N than nitrate and nitrite. Therefore, NH_4^+-N becomes the preferential source of nitrogen for microalgae. NH_4^+-N present in effluents is transported into the cell by an ammonium transporter. Microalgal species utilise NH_4^+-N and finally convert it to L-Glutamate, which further converts into biomass (Singh and Mishra 2019). Hence, biomass productivity can be directly correlated with ammonium nitrogen removal. **Table 3.4** represents the comparative evaluation of *D. mucosa* VSPA and *C. pyrenoidosa* for the assimilation of NH_4^+-N from different wastewater sources. It is evident from **Table 3.4** that *D. mucosa VSPA* outperformed *C. pyrenoidosa* in all wastewater sources ($p < 0.05$). Due to the two-day lag phase, there was a slight decrease in ammonium removal due to the dependency of nutrient removal on microalgae growth. But after the second day, the NH_4^+-N concentration rapidly decreased until day 10. The highest ammonium removal efficiency was obtained by *D. mucosa* VSPA in carpet effluent (94%)

during the 10-day cultivation period, while it was 87.97% for *C. pyrenoidosa* in the same effluent. Carpet industrial units in Bhadohi, India (popularly known as the Carpet Capital of India), alone generate 7% of the total wastewater generated in the city [280]. Therefore, *D. mucosa* species will be beneficial for carpet effluent treatment. Chinnasamy et al. (2010) cultivated 15 native algal isolates in a medium containing carpet industry effluent. The treatment method was highly effective, and more than >96% of pollutants were remediated [281].

Table 3.4. Ammonium nitrogen removal efficiency obtained during the cultivation of *D. mucosa* VSPA and *C. pyrenoidosa* in different effluents.

Wastewater Source	***D. mucosa* VSPA**			***C. pyrenoidosa***		
	Initial Conc. (mg/L)	Final Conc. (mg/L)	Removal efficiency (%)	Initial Conc. (mg/L)	Final Conc. (mg/L)	Removal efficiency (%)
TE1	45.2±0.16	4.34±0.07	90.4±0.20	45.2±0.16	7.34±0.07	83.8±0.20
TE2	54.6±0.81	5.34±0.07	90.2±0.10	54.6±0.81	8.67±0.41	84.1±1.00
TE3	46.2±0.69	8.00±0.53	82.7±1.00	46.2±0.69	10.34±0.07	77.63±0.30
Carpet Effluents	83.8±0.82	7.36±0.86	91.2±1.50	83.8±0.82	11.69±0.47	86.0±0.70

Among the three variants of textile effluent, the highest NH_4^+-N removal efficiency of 90.4 ± 0.2% was obtained in TE1 by *D. mucosa VSPA* during a 10-days cultivation period. A slightly lower RE of 90.2 ± 0.1% was obtained in TE2, and the lowest RE of 82.7 ± 1.0 % was obtained in TE3. In the case of *C. pyrenoidosa*, the highest RE of 84.1 ± 1.0 % was obtained in the case of TE2, with subsequent RE of 83.8 ± 0.2 % in TE1 and 77.63 ± 0.3 % in TE3. RE in the TE3 for both species was lower than other wastewater sources, possibly due to the low N/P ratio or more toxic compounds. Brar et al. (2019) cultivated three microalgal species, *Chlorella pyrenoidosa, Scenedesmus abundans, and Anabaena*

ambigua, in 75% diluted textile effluent. Species were cultivated for 25 days, and 74.43% RE for nitrogen was obtained by *C. pyrenoidosa*, and 70.79% RE was obtained by *S. abundans* [282]. It is possible that a significant amount of NH_4^+-N may be removed due to biological processes, such as bacterial nitrification, or physical processes, such as volatilization or sedimentation[283], [284]. But, in the control experiment, less than 10% of NH_4^+-N was removed, indicating that microalgae were solely responsible for removing a significant percent of NH_4^+-N.

3.3.2.2. Phosphate-phosphorus (PO_4^{3-}-P) Removal Efficiency (PRE)

Phosphorus present in wastewater is of two types: organic and inorganic. Inorganic phosphorus, or phosphate phosphorus (PO_4^{3-}-P), is transported into the cytosol by a specific transporter[285]. In the cytosol, phosphate phosphorus can be converted into nucleic acid, protein, or insoluble granules, as shown in **Figure 3.6**. Hence, phosphorus is indirectly related to biomass production. **Table 3.5** compares *D. mucosa* VSPA and *C. pyrenoidosa* for assimilating PO_4^{3-}-P from different wastewater sources.

Table 3.5. Phosphate phosphorus removal efficiency obtained during the cultivation of *D. mucosa VSPA* and *C. pyrenoidosa* in different effluents.

Wastewater Source	***D. mucosa* VSPA**			***C. pyrenoidosa***		
	Initial Conc. (mg/L)	Final Conc. (mg/L)	Removal efficiency (%)	Initial Conc. (mg/L)	Final Conc. (mg/L)	Removal efficiency (%)
TE1	5.47±0.12	1.63±0.05	70.1±0.56	5.47±0.12	1.92±0.04	64.9±0.50
TE2	6.43±0.12	1.82±0.09	71.6±1.80	6.43±0.12	2.14±0.05	66.7±1.00
TE3	7.8±0.08	2.43±0.12	68.8±1.92	7.8±0.12	2.9±0.25	62.8±3.30
Carpet Effluents	9.37±0.17	2.6±0.08	71.6±1.90	9.37±0.17	3.13±0.05	66.7±1.00

In this case, also, *D. mucosa* VSPA outperformed *C. pyrenoidosa* in all effluents, representing a better strain for the effluent treatment ($p < 0.05$). The efficiency of PO_4^{3-}-P removal by microalgae was less than that of NH_4^+-N because of the straightforward fact that the requirement of nitrogen by microalgae is greater; in contrast, only 1% (by weight) phosphate is present in algae biomass [286], [287]. It has also been reported that species belonging to the *Trebouxiophyceae* class can assimilate excess PO_4^{3-}-P present in the medium and store it in their vacuoles as polyphosphate granules. These granules can be used later in phosphorus-deficient conditions [287].

In carpet effluent, *D. mucosa* VSPA removed 71.6 ± 1.9 % of PO_4^{3-}-P, while *C. pyrenoidosa* was able to remove 66.7 ± 1.0 % of PO_4^{3-}-P. The final concentration of PO_4^{3-}-P reached 2.6 ± 0.08 mg/L in the case of *D. mucosa* VSPA and 3.13 ± 0.05 mg/L in the case of *C. pyrenoidosa* within 10 days of the cultivation period. Among the three variants of textile wastewater, similar to the case of ammonium nitrogen, the lowest PRE of 68.8 ± 1.92 % and 62.8 ± 3.3 % was obtained in the case of TE3 by *D. mucosa VSPA* and *C. pyrenoidosa*, respectively. At the same time, the highest PRE was obtained in TE2 by both species. They removed 71.6 ± 1.8 % and 66.7 ± 1.0 % phosphate, respectively. Brar et al. (2019) cultivated *C. pyrenoidosa* and *S. abundans* in 75% diluted textile wastewater for 25 days under batch conditions. *C. pyrenoidosa* was able to remove only 28.01% PO_4^{3-}-P, significantly less than the present case (Brar et al. 2019b). Similar to the case of NH_4^+-N, some portion of PO_4^{3-}-P may be eliminated due to some physical processes, such as chemical precipitation[288]. However, here also, less than 10% of PO_4^{3-}-P was eliminated in the control experiment, indicating that microalgae assimilated a significant portion of phosphate.

3.3.2.3. COD Removal Efficiency (CRE)

Chemical oxygen demand (COD), a measurement of the organic load (strength of the effluent) in the wastewater and the amount of molten oxygen that may be used for its

oxidation, is another key element in wastewater treatment [289]. In contrast to other common nutrients like nitrogen and phosphorus, the fate of COD during microalgal-based wastewater treatment has not been extensively characterised [290]. The organic carbon is first transported to the cytosol by a specific transporter. Then, it is converted to L -glutamate and carbohydrate by the carbon centrate mechanism. Carbohydrate is used for energy production, and L- glutamate is used for biomass production, as shown in **figure 3.6**. Hence, COD removal can be directly correlated with biomass production. Both species were compared for their COD removal efficiency in all effluents, and the obtained results are presented in **Table 3.6**. A general trend can be observed: as the COD concentration increased, COD removal efficiency also increased. As the highest COD was detected in carpet effluent (1568 ± 14 mg/L), both species' highest COD removal efficiency was obtained in carpet effluent. *D. mucosa* VSPA removed 91.9 ± 0.4% of COD, and 87.1 ± 0.9% of COD was removed by *C. pyrenoidosa*. The final concentration reached 126.70 ± 5.25 mg/L in *D. mucosa* VSPA culture, and 202.7 ± 13.1 mg/L in the case of *C. pyrenoidosa*. Notably, this is the first publication that reports COD removal from carpet effluent by microalgae.

Table 3.6. COD removal efficiency obtained during the cultivation of *D. mucosa VSPA* and *C. pyrenoidosa* in different effluents.

Wastewater Source	***D. mucosa* VSPA**			***C. pyrenoidosa***		
	Initial Conc. (mg/L)	Final Conc. (mg/L)	Removal efficiency (%)	Initial Conc. (mg/L)	Final Conc. (mg/L)	Removal efficiency (%)
TE1	394±4.30	81±8.04	79.4±2.20	394±4.30	105±2.50	73.3±0.90
TE2	372±3.20	70±3.20	81.2±0.70	372±3.20	95±2.50	74.4±0.80
TE3	438±8.16	104.6±6.18	76.1±1.60	438±8.16	122.3±7.85	72.1±2.10

Carpet Effluents	1568±14.70	126.7±5.25	91.9±0.40	1568±14.70	202.7±13.10	87.1±0.90

In the case of textile effluent, like other pollutants, the highest COD RE was obtained in TE2. In comparison, the lowest was obtained in TE3. *D. mucosa VSPA* eradicated 81.2 ± 0.7% COD, while *C. pyrenoidosa* eradicated 74.4 ± 0.8% from the TE2. The results were analogous to the previously reported findings. Wu et al. (2020) cultivated immobilised *Chlorella* sps. in different concentrations of textile wastewater in glass tubes. All species were able to remediate more than 75% of COD from the textile effluent[291]. In another study, Behl et al. (2020) remediated effluent from a textile dyeing mill with an isolated *Chlamydomonas* sp. TRC-1. Complete colour removal was obtained within 7 days, with a COD removal efficiency of 83.08% [292]. The release of organic molecules by microalgal cells will undoubtedly cause the COD of the sample to rise when the culture enters the stationary phase. However, high removal efficiency in both cultures suggested that some COD may have been remedied by bacterial contamination, as shown in the control, or that newly forming microalgal cells may have assimilated the released organic content. A summarised table comparing the efficiency of both species for the treatment of textile and carpet effluent is presented in **Table 3.7.**

Table 3.7. Comparison of biomass production and pollutant removal efficiency by *D. mucosa* VSPA and *C. pyrenoidosa*.

Wastewater Source	**Microalgae Species**							
	***D. mucosa* VSPA**				***C. pyrenoidosa***			
		Removal Efficiency (%)				**Removal Efficiency (%)**		
	Biomass Conc. (g/L)	**NH_4^+-N**	**PO_4^{3-}-P**	**COD**	**Biomass Conc. (g/L)**	**NH_4^+-N**	**PO_4^{3-}-P**	**COD**
TE1	3.98±0.4	90.4±1.0	70.1±1.3	79.4±1.4	3.31±0.2	83.8±±1.5	64.9±1.3	73.3±1.4

TE2	3.85±0.31	90.2±1.5	71.6±1.7	81.2±1.3	3.00±0.4	84.1±1.5	66.7±0.9	74.4±1.9
TE3	2.90±0.39	82.7±2.4	68.8±0.9	76.1±2.2	2.28±0.2	77.63±1.6	62.8±1.9	72.1±1.3
Carpet Effluent	4.26±0.45	94.0±1.8	71.6±1.3	91.9±1.9	4.02±0.3	87.9±2.5	66.7±1.7	87.1±1.4

3.3.3. Colour Removal Efficiency

The primary source of colour in wastewater is dyes, particularly in carpet and textile effluents. Figure 4 represents the mechanism through which microalgae remediate dye from wastewater.

As depicted in **Figure 3.7,** microalgal cells remediate colour from wastewater generally through four processes: (i) biodegradation; (ii) bioadsorption; (iii) bioaccumulation; and (iv) biotransformation. In biodegradation, dyes such as azo dyes are degraded by azoreductase enzyme into colourless and non-toxic amines [294]. In the bio-adsorption process, dyes are adsorbed on the cell surface due to opposite charge polarities on the cell surface and dyes [293]. Next, in the bioaccumulation process, dyes are converted into simpler carbon compounds via some enzyme, such as laccase [293]. Later, these compounds are metabolised by algal cells. Last, in the biotransformation process, the peroxidase enzyme transforms dye into non-toxic molecules [295]. **Table 3.8** represents the colour removal efficiency of various effluents.

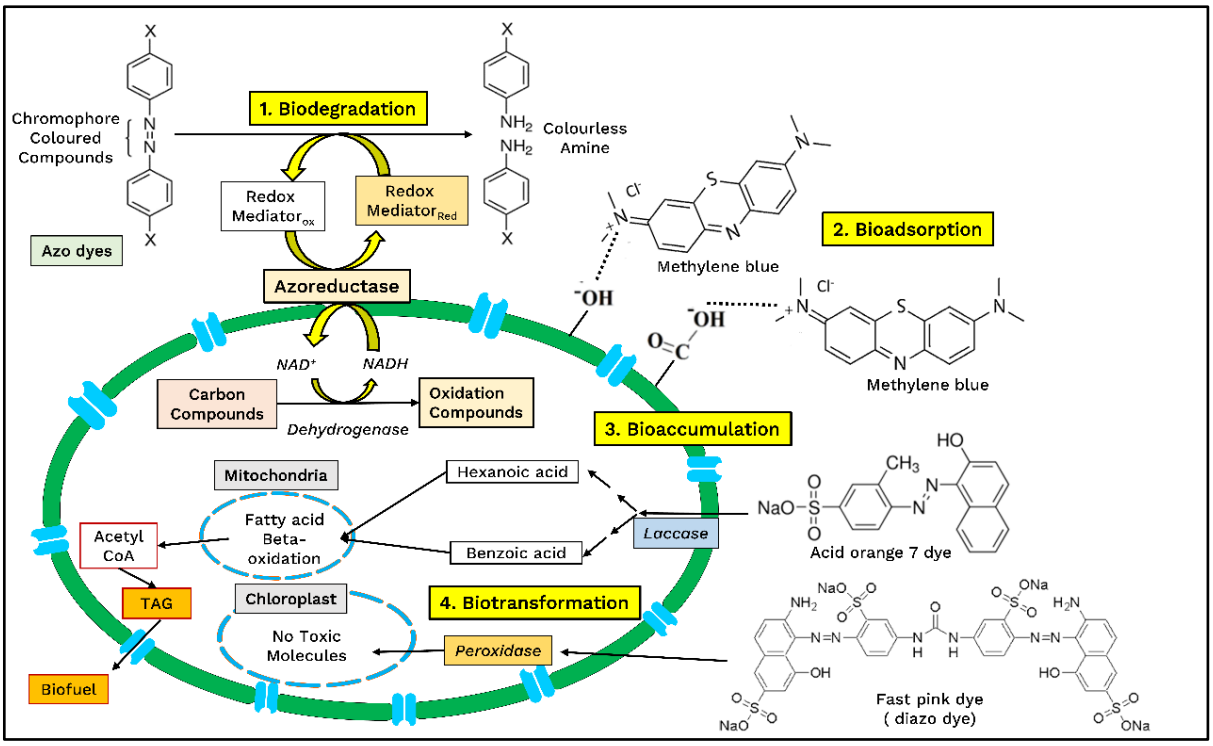

Figure 3.7. Schematic diagram representing colour removal by microalgae via four mechanisms: (1) Biodegradation (degradation into simpler compounds); (2) Bio adsorption (adsorption on the cell surface); (3) Bioaccumulation (conversion into simpler compounds and storage in cells for later use); (4) Biotransformation (transformation into non-toxic compounds)[293]–[295].

As per the mechanism, it is clear that more growth will favour more colour removal. The highest colour removal was obtained in TE2 by both species, which was 67.00 ± 1.90% in *D. mucosa* VSPA culture, while 62.90 ± 0.96% removal was obtained in *C. pyrenoidosa* culture. The lowest was obtained in the TE3, which was 54.70 ± 1.55% in *D. mucosa* VSPA, while removal efficiency reached 49.10 ± 0.71% in *C. pyrenoidosa* culture. In the remaining effluents (carpet, domestic, and petroleum), more than 70% colour removal efficiency was obtained in the *D. mucosa* VSPA culture. In comparison, more than 65% colour remediation was obtained in *C. pyrenoidosa* cultures.

Table 3.8. Colour removal efficiency obtained during the cultivation of *D. mucosa VSPA* and *C. pyrenoidosa* in different effluents.

Wastewater Source	*D. mucosa* VSPA			*C. pyrenoidosa*		
	Initial Conc. (mg/L)	Final Conc. (mg/L)	Removal efficiency (%)	Initial Conc. (mg/L)	Final Conc. (mg/L)	Removal efficiency (%)
TE1	140±2.00	49±1.00	65.5±2.14	140±2.30	56±1.00	60.9±1.30
TE2	180±3.10	59±1.00	67.0±1.90	180±.20	66±2.21	62.9±0.96
TE3	200±4.20	110±2.00	54.7±1.55	200±3.10	102±3	49.1±0.71
Carpet Effluents	95±2.00	29±1.00	69.2±2.14	95±1.10	34±1.30	64.7±2.01

3.3.4. Modelling Study

Two models, the PhBT and Gompertz models, were used for modelling the study and validating the experimental results. In addition to R^2 values, AICC values are used to compare theoretical models better. **Table 3.9** and **Figure 3.8** represent the modelling simulation study for biomass production.

Table 3.9. Kinetic parameters and AICC values obtained after biomass simulation study.

Microalgae Species	Wastewater Source	Model	Kinetic Parameters	R^2	Adj. R^2	RMSE	AICC
Diplosphaera mucosa VSPA	TE1	PhBT	$p = 0.45\ d^{-1}$	0.96	0.96	1.24	7.61
		Gompertz	$\lambda = 0.47$ d $\mu_m = 0.65\ d^{-1}$	0.94	0.94	0.56	14.12
	TE2	PhBT	$p = 0.47\ d^{-1}$	0.98	0.98	0.95	-3.78

		Gompertz	$\lambda = 1.33$ d $\mu_m = 0.56$ d^{-1}	0.94	0.94	0.56	2.81
	TE3	PhBT	p = 0.39 d^{-1}	0.98	0.98	0.60	-15.87
		Gompertz	$\lambda = 0.17$ d $\mu_m = 0.37$ d^{-1}	0.97	0.97	0.60	-3.57
	Carpet	PhBT	p = 0.59 d^{-1}	0.98	0.98	0.92	-4.57
		Gompertz	$\lambda = 0.87$ d $\mu_m = 0.60$ d^{-1}	0.97	0.97	0.99	6.4
Chlorella pyrenoidosa	TE1	PhBT	p = 0.56 d^{-1}	0.94	0.94	0.46	7.56
		Gompertz	$\lambda = 0.29$ d $\mu_m = 0.58$ d^{-1}	0.92	0.91	0.50	13.93
	TE2	PhBT	p = 0.49 d^{-1}	0.98	0.98	0.53	-8.48
		Gompertz	$\lambda = 0.29$ d $\mu_m = 0.58$ d^{-1}	0.92	0.91	0.50	13.93
	TE3	PhBT	p = 0.49 d^{-1}	0.95	0.95	0.38	-4.62

	Gompertz	$\lambda = 0$ d $\mu_m = 0.36$ d^{-1}	0.93	0.92	0.44	3.62
Carpet	PhBT	p = 0.54 d^{-1}	0.96	0.95	0.43	9.92
	Gompertz	$\lambda = 0.49$ d $\mu_m = 0.66$ d^{-1}	0.94	0.94	0.58	14.38

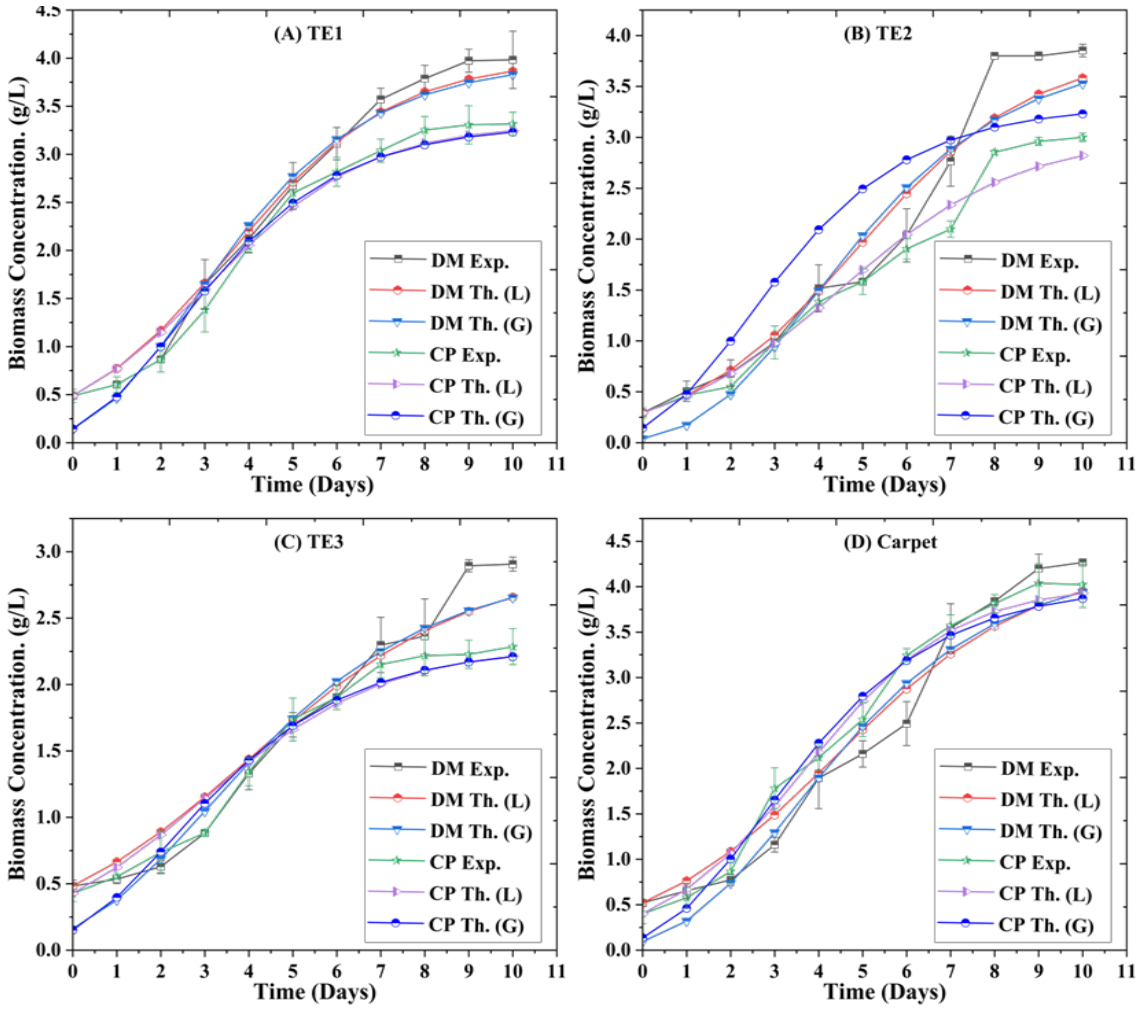

Figure 3.8. Model simulation results obtained for biomass production: (A) Textile effluent 1 (TE1); (B) Textile effluent 2 (TE2); (C) Textile effluent 3 (TE3); (D) Carpet effluent; (DM: *D. mucosa* VSPA; CP: *Chlorella pyrenoidosa*; Exp.: Experimental Concentration;

Th. (L) & Th. (G): Theoretical concentration obtained from Photobiotreatment and Gompertz models). The photobiotreatment model was a better fit model than Gompertz model.

R^2 and RMSE (Root Mean Square Error) values indicated that both models better fitted the experimental results. But, AICC values indicate that the PhBT model provides a better fit than the Gompertz model. Maximum specific growth (p), as revealed by the PhBT model, was highest in carpet effluent for both species and lowest in TE3. It was even higher for the *D. mucosa* VSPA strain. The results of kinetic parameters were reflected in biomass concentration results, as the highest biomass concentration was obtained in carpet effluent. p is one of the critical parameters for deciding the dilution rate and flow rate during the design of a continuous reactor. Also, as revealed by the Gompertz model, the lag phase duration was low in carpet effluent compared to textile effluent. Model simulation studies for nutrient removal is represented in **Tables 3.10 and 3.11** and **Figures 3.9 and 3.10**, respectively.

Table 3.10. Kinetic parameters and AICC values obtained after ammonium nitrogen removal simulation study.

Microalgae Species	**Wastewater Source**	**Model**	**Kinetic Parameters**	**R^2**	**Adj. R^2**	**RMSE**	**AICC**
Diplosphaera mucosa VSPA	TE1	PhBT	$p = 0.70\ d^{-1}$ $Y = 0.07$ mg/g	0.90	0.89	3.95	77.70
		Gompertz	$\lambda = 0.87$ d $k = 0.60\ d^{-1}$	0.89	0.88	0.56	79.28
	TE2	PhBT	$p = 0.81\ d^{-1}$	0.89	0.88	2.08	51.54

			Y = 0.16 mg/g				
		Gompertz	λ = 0.28 d μ_m = 1 d^{-1}	0.98	0.98	11.68	73.90
	TE3	PhBT	p = 0.74 d^{-1} Y = 0.13 mg/g	0.93	0.92	3.77	77.27
		Gompertz	λ = 0.31 d k = 1 d^{-1}	0.98	0.98	14.97	62.92
	Carpet	PhBT	p = 0.64 d^{-1} Y = 0.06 mg/g	0.97	0.93	7.50	77.27
		Gompertz	λ = 0.36 d k = 1 d^{-1}	0.96	0.96	23.85	62.92
Chlorella pyrenoidosa	TE1	PhBT	p = 0.86 d^{-1} Y = 0.23 mg/g	0.91	0.90	2.38	76
		Gompertz	λ = 1.5 d k = 0.65 d^{-1}	0.91	0.92	0.50	2.13
	TE2	PhBT	p = 0.81 d^{-1} Y = 0.16 mg/g	0.98	0.96	2.08	45.89
		Gompertz	λ = 1 d k = 0.28 d^{-1}	0.89	0.87	11.68	72.33
	TE3	PhBT	p = 0.74 d^{-1}	0.93	0.92	3.77	54.67

			Y = 0.13 g/mg				
		Gompertz	λ = 1 d k = 0.31 d^{-1}	0.98	0.98	14.97	73.95
	Carpet	PhBT	p = 0.69 d^{-1}	0.94	0.94	7.43	54.67
			Y = 0.07 g/mg				
		Gompertz	λ = 0.29 d k = 1 d^{-1}	0.98	0.98	21.41	73.95

Table 3.11. Kinetic parameters and AICC values obtained after phosphate phosphorus removal simulation study.

Microalgae Species	**Wastewater Source**	**Model**	**Kinetic Parameters**	**R^2**	**Adj. R^2**	**RMSE**	**AICC**
Diplosphaera mucosa VSPA	TE1	PhBT	p = 0.84 d^{-1} Y = 2.39 g/mg	0.91	0.90	0.29	21.52
		Gompertz	λ = 1.40 d k = 0.65 d^{-1}	0.90	0.89	0.14	22.37
	TE2	PhBT	p = 0.66 d^{-1} Y = 1.76 g/mg	0.96	0.96	0.36	15.05
		Gompertz	λ = 1.59 d k = 0.51 d^{-1}	0.95	0.95	0.42	17.40

	TE3	PhBT	p = 0.64 d^{-1} Y = 1.44 g/mg	0.96	0.96	0.59	16.81
		Gompertz	λ = 1.58 d k = 1.58 d^{-1}	0.96	0.95	0.69	19.43
	Carpet	PhBT	p = 0.68 d^{-1} Y = 1.38 mg/g	0.94	0.93	0.50	23.86
		Gompertz	λ = 1.65 d k = 0.52 d^{-1}	0.95	0.95	0.47	26.28
Chlorella pyrenoidosa	TE1	PhBT	p = 0.81 d^{-1} Y = 3.35 mg/g	0.93	0.93	0.33	16.51
		Gompertz	λ = 1.67 d k = 0.62 d^{-1}	0.93	0.92	0.34	17.93
	TE2	PhBT	p = 0.78 d^{-1} Y = 4.44 mg/g	0.99	0.99	0.17	15.91
		Gompertz	λ = 2.2 d k = 0.57 d^{-1}	0.95	0.94	0.27	17.91
	TE3	PhBT	p = 0.74 d^{-1} Y = 0.13 g/mg	0.83	0.80	5.09	13.47
		Gompertz	λ = 1.53 d k = 0.45 d^{-1}	0.97	0.96	0.39	36.41

	Carpet	PhBT	p = 0.65 d^{-1}	0.93	0.92	0.57	20.27
			Y = 1.14 g/mg				
		Gompertz	λ = 1.75 d	0.96	0.95	0.53	23.31
			k = 0.50 d^{-1}				

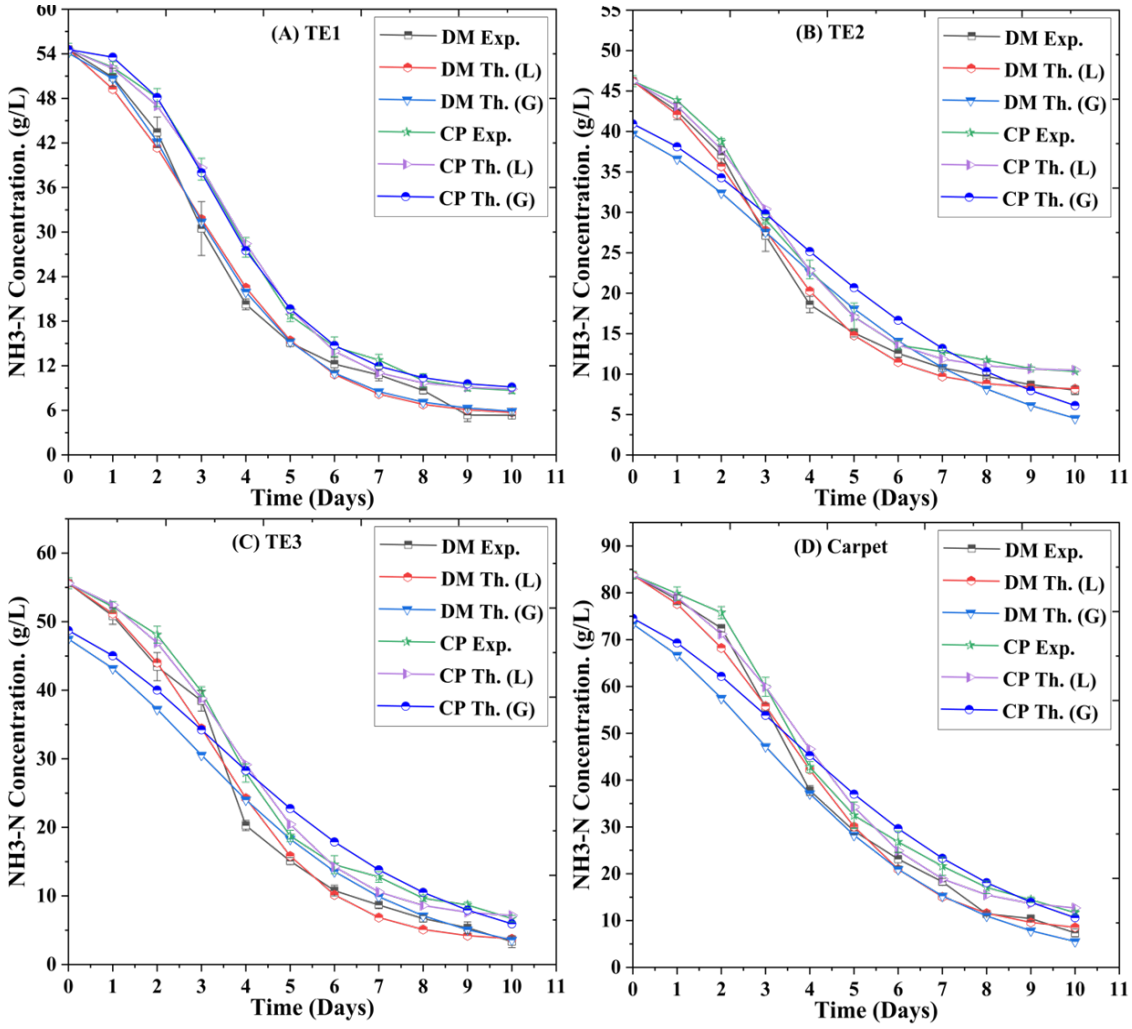

Figure 3.9. Model simulation results obtained for ammonium nitrogen removal: (A) Textile effluent 1 (TE1); (B) Textile effluent 2 (TE2); (C) Textile effluent 3 (TE3); (D) Carpet effluent; (DM: *D. mucosa* VSPA; CP: *Chlorella pyrenoidosa*; Exp.: Experimental Concentration; Th. (L) & Th. (G): Theoretical concentration obtained from Photobiotreatment and Gompertz models. Here also, the photobiotreatment model was a better fit model than Gompertz model.

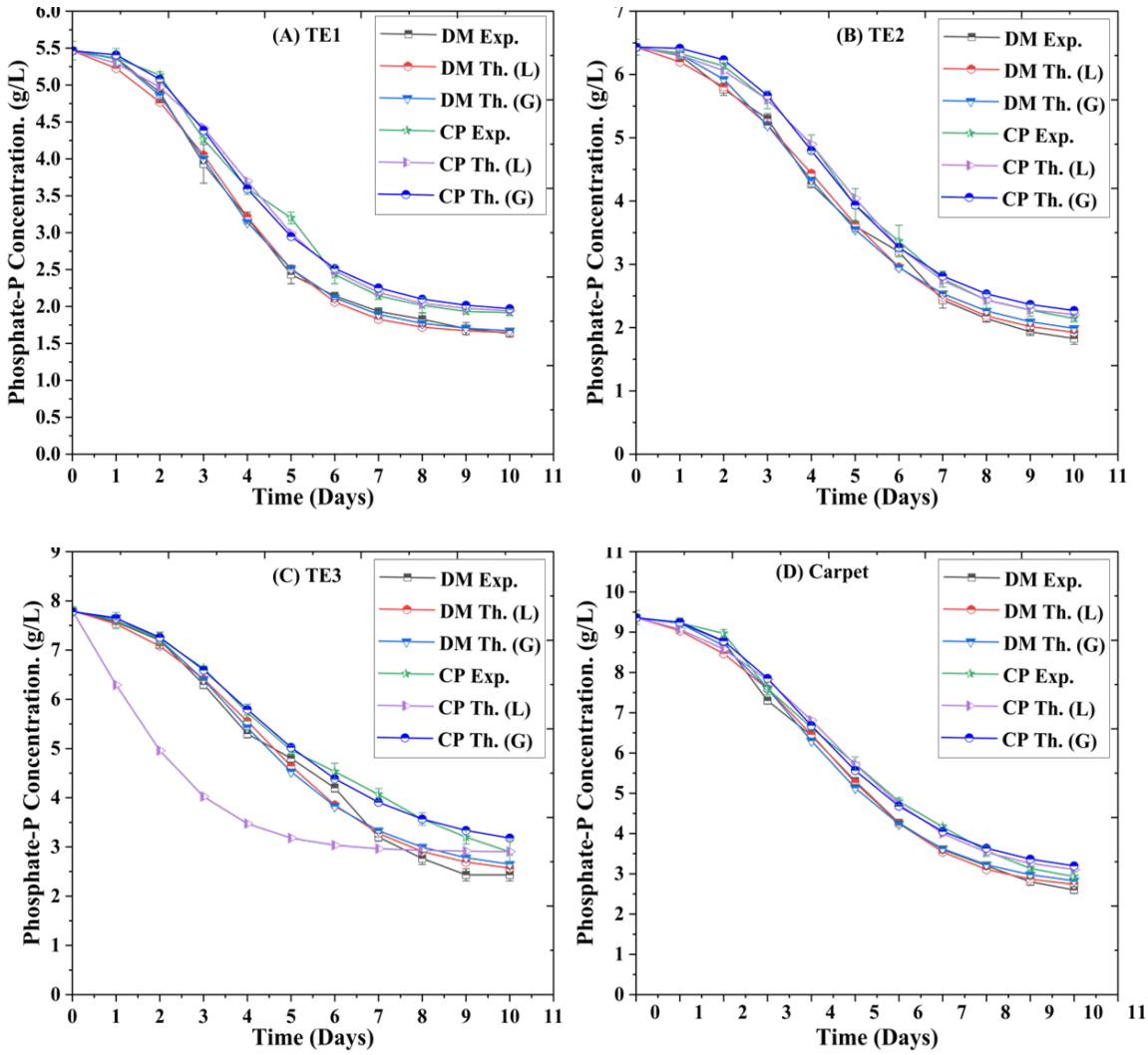

Figure 3.10. Model simulation results obtained for phosphate phosphorus removal: (A) Textile effluent 1 (TE1); (B) Textile effluent 2 (TE2); (C) Textile effluent 3 (TE3); (D) Carpet effluent; (DM: *D. mucosa* VSPA; CP: *Chlorella pyrenoidosa*; Exp.: Experimental Concentration; Th. (P) & Th. (G): Theoretical concentration obtained from Photobiotreatment and Gompertz models. Here also, the photobiotreatment model was a better fit model than Gompertz model.

Here, too, the AICC value indicated that the PhBT model better fits the experimental data of pollutant removal compared to the Gompertz model. p values obtained during the model simulation study also indicate that the *D. mucosa VSPA* strain has a high growth rate. Even if the investigated nutrient is not limiting, the PhBT model can still be used for nitrogen and phosphorus. Although it hasn't been empirically proven in this study,

theoretically, the model might be used for any nutrient readily available in a finite concentration. The PhBT model can calculate the maximum number of nutrient reserves throughout the experiment and the microalgae's luxurious uptake of nutrients. Consideration should be given to implementing a suitable cultivation mode during wastewater treatment, where the primary goal is the removal of nutrients rather than maximising biomass production [296]. In some cases, the Gompertz model also provided a better fit to the experimental data. This might indicate a chance of nutrient removal through physical processes such as adsorption by microalgae biomass.

3.4. Conclusion

In the present study, two microalgal strains, *D. mucosa VSPA* and *C. pyrenoidosa, were* compared for their growth and treatment efficiency of textile and carpet effluent cultivated in conventionally designed bubble column PBR. *D. mucosa VSPA* proved to be a superior strain than *C. pyrenoidosa*, with the final biomass concentration reaching 4.26 g/L in carpet effluent. Current treatment technology provides better removal efficiency of pollutants, including more than 85% removal of ammonium nitrogen, 70% of phosphate phosphorus, 75% of COD, and 60% of colour from all effluent. The PhBT model better fits the experimental data, providing some critical design parameters. The study can be expanded by testing more unexplored microalgae strains to treat various industrial effluents. Dumping points in industries can be a potential source of unexplored strains. Also, the discussed design parameters of the bubble column reactor will assist future studies in the easy scale-up of the photobioreactors.